Journal of Invertebrate Pathology 136 (2016) 81–91

Contents lists available at ScienceDirect

Journal of Invertebrate Pathology

journal homepage: www.elsevier.com/locate/jip

Microsporidia *Alfvenia sibirica* sp. n. and *Agglomerata cladocera* (Pfeiffer) 1895, from Siberian microcrustaceans and phylogenetic relationships within the "Aquatic outgroup" lineage of fresh water microsporidia

Y.Y. Sokolova [a,c,*], I.V. Senderskiy [b], Y.S. Tokarev [b]

[a] Institute of Cytology, Russian Academy of Sciences, St. Petersburg, Russia
[b] All-Russia Institute for Plant Protection, Russian Academy of Sciences, St. Petersburg, Russia
[c] Department of Comparative Biological Sciences, School of Veterinary Medicine, Louisiana State University, Baton Rouge, LA, USA

ARTICLE INFO

Article history:
Received 25 November 2015
Revised 17 February 2016
Accepted 14 March 2016
Available online 15 March 2016

Keywords:
Microsporidiosis
Copepoda
Cladocera
Cyclopidae
Daphnia
Ultrastructure
Molecular phylogeny

ABSTRACT

Here we report on two microsporidia from freshwater crustaceans collected during the ongoing survey for microsporidia in the river Karasuk and adjacent waterbodies (Novosibirsk region, Western Siberia). The first species parasitized hypoderm and fat body of a cyclopid *Cyclops* sp. (Maxillopoda, Copedoda) and produced oval spores, measured 2.0 × 3.6 μm (fixed) enclosed individually or in small groups in fragile sporophorous vesicles (SVs). We describe it here as *Alfvenia sibirica* sp. n. The second species infected the same tissues of a cladoceran *Daphnia magna* (Branchiopoda, Phyllopoda). Its spores were pyriform, 2.3 × 4.0 μm (fixed), and resided in relatively persistent SVs in groups of 8–16. This species was identified as a Siberian isolate (Si) of *Agglomerata cladocera* (Pfeifer) because ultrastructurally it was hardly distinguishable from *A. cladocera* recorded from England from the same host (Larsson et al., 1996). *A. cladocera* (Si) shared 99% SSU rDNA sequence similarity to *Binucleata daphniae* from *D. magna* collected in Belgium (Refardt et al., 2008). The major outcome of our work is that we present molecular (SSUrDNA) characterization coupled with EM description, for representatives of two genera, *Alfvenia* (encompasses 3 described so far species) and *Agglomerata* (7 species), which allowed us to place these two genera on the phylogenetic tree. We also summarized the literature data on *Alfvenia* and *Agglomerata* spp., and provided their comparative morphological analysis. These two genera belong to so called "Aquatic outgroup" (Vossbrinck et al., 2004), a poorly resolved lineage, a sister to Amblyosporidae. This lineage probably includes majority of fresh water forms of microsporidia, most of which remain undescribed. SSUrDNA-based phylogenetic analysis and analysis of hosts suggest that diversification within the "Aquatic outgroup" could have been connected with the host switch from dipterans or copepods to cladocerans that had occurred in some ancestral *Amblyospora*-related lineage(s).

© 2016 Elsevier Inc. All rights reserved.

1. Introduction

During the ongoing survey for microsporidia in the river Karasuk and adjacent water bodies in Western Siberia we discovered two microsporidia species that infect freshwater crustaceans. The first species was isolated from a cyclopid *Cyclops* sp. (Maxillopoda, Copedoda) and morphologically resembled representatives of the genus *Alfvenia* (Vidtmann and Sokolova, 1995). The second species infected a cladoceran *Daphnia magna* (Branchiopoda, Phyllopoda) and shared structural similarities with *Agglomerata cladocera* (Larsson et al., 1996). Representatives of both genera were recorded previously from Europe. The initial goal of the research was to describe fine morphology of the discovered microsporidia, identify the species, and determine their relationships with other taxa of the phylum Microsporidia by comparative ultrastructural and SSU rDNA-based phylogenetic analyses. Obtaining SSU rDNA sequences for representatives of two genera *Alfvenia* and *Agglomerata*, allowed us to place these two genera on the phylogenetic tree within the so-called "Aquatic outgroup" (sensu Vossbrinck et al., 2004), a poorly resolved lineage, a sister to Amblyosporidae. This lineage probably includes majority of fresh water forms of microsporidia, most of which remain undescribed. We also provide a comparative morphological analysis of the representatives of the genera *Alfvenia* and *Agglomerata*.

* Corresponding author at: Microscopy Center, Department of Comparative Biological Sciences, School of Veterinary Medicine, Louisiana State University, 1909 Skip Bertman Drive, Baton Rouge, LA 70803, USA.
E-mail address: sokolova@lsu.edu (Y.Y. Sokolova).

http://dx.doi.org/10.1016/j.jip.2016.03.009
0022-2011/© 2016 Elsevier Inc. All rights reserved.

2. Material and methods

2.1. Sampling

The crustaceans were collected in the lake Krotova Lyaga belonging to the river Karasuk basin, Karasuk District of Novosibirsk region, South-Western Siberia (56°32′N, 29°31′E) in May and June in 2013 and 2014. In May 2013, water fleas *D. magna* were abundant in the lake, with significant proportion of organisms exhibiting pathology characteristic for microsporidiosis. In June 2014, a single heavily infected adult of *Cyclops* sp. was collected. Transformation of its habitus due to infection did not allow identification of species. The smears of infected crustaceans were immediately fixed with methanol, for consequent light microscopy (LM) examination. Infected animals were cut in halves. One half was placed in 2.5% glutaraldehyde in 0.1 M cacodylate buffer to be processed further for electron microscopy, another – in 95% ethanol to be used for DNA extraction. Samples were stored at 4 °C until further processing.

2.2. Electron microscopy

For transmission electron microscopy (TEM), in about 2 weeks after fixation, the samples were cut in smaller pieces, transferred to fresh portion of fixative for 2 h, washed in 0.1 M cacodylate buffer supplemented with 5% sucrose, post fixed in 2% osmium tetroxide, dehydrated in ascending ethanol series, transferred to propylene-oxide, and embedded in Epon-Araldite. Thick (0.5–1 μm) sections were stained with Methylene blue, examined and photographed under Zeiss Axioplan microscope equipped with Olympus DP73 digital camera and CellSens (Version 510) software. Thin (70–80 nm) sections were stained with uranyl acetate and Reynolds' lead citrate end examined in JEOL JEM 1011 transmission electron microscope equipped with HAMAMATSU ORCA-HR digital camera (Tokyo, Japan).

For Scanning electron microscopy (SEM), specimens were fixed with glutaraldehyde only, dehydrated through the ethanol series, followed by exchanging ethanol with CO_2 in Polaron E3000 Standard Critical Point Drier. Dried samples were mounted on 13 mm aluminum mount specimen stubs covered with carbon adhesive tabs, sealed with colloidal silver paste, coated with Gold/Palladium in EMS 550X Sputter Coater for 4 min to achieve the thickness of coating 20–25 nm., and examined in Fei Quanta 200 ESEM in a high vacuum mode at 20 kV. All reagents for LM were from SIGMA-ALDRICH (St. Louis, MO), and for EM – from EMS Chemicals (Fort Washington, PA).

2.3. DNA sequencing

Ethanol-fixed samples were transferred to new tubes and left to air dry. After ethanol evaporation, samples were homogenized with a plastic pestle in 100 μl lysis buffer (2% cetrimonium bromide, 1.4 M NaCl, 100 mM EDTA and 100 mM Tris–Cl (pH 8.0)). Another 500 μl of lysis buffer containing 0.2% β-mercaptoethanol and 10 μl proteinase K (20 mg mL^{-1}) were added to each tube. The samples were then incubated at 65 °C for 3 h. DNA was extracted routinely with phenol-chloroform (Sambrook et al., 1989) and re-suspended in 50 μl UHQ water. The small subunit (SSU) rRNA gene was amplified by the 18f-1047r primer set (Weiss and Vossbrinck, 1999).

PCR was run using MyCycler (Bio-Rad) in 20 μl volume containing 10 μl tenfold-diluted DNA template; 2 μl PCR buffer with 25 mM $MgCl_2$; 1 μl dNTPs, 0.25 mM; 0.5 μl Taq-polymerase (2500 U mL^{-1}, Sileks, Russia); 1 μl of each forward and reverse 10 μM primers (Evrogen, Russia). Initial denaturation was carried out at 92 °C for 3 min, followed by 30 cycles of denaturation at 92 °C for 30 s, annealing at 54 °C for 30 s, and elongation at 72 °C for 30 s, and final extension at 72 °C for 10 min. The PCR products of about 900 bp long were gel-purified and sequenced in both directions using ABI Prism 3500 (Applied Biosystems). The obtained sequence reads were manually corrected and assembled using BioEdit software (Hall, 1999).

For host identification, additional PCRs were performed using primer sets LepF1:LepR1 (Hebert et al., 2004) specific for COI region of a broad range of Metazoa, and f1300:ITS2-28S specific for rRNA in Eukarya (Navajas et al., 1998). The conditions for reactions were as described above. COI region was successfully amplified for the water flea. The obtained sequence was 98–100% identical to those available in Genbank for *Daphnia magna* and below 96% for other *Daphnia* species. This allowed host identification as *D. magna*, supporting the routine identification with the field guide. Genomic DNA extracted from the infected cyclopid could not be amplified with the host-targeted primers. The genus (*Cyclops*) was identified using the conventional field guide (Tsalolihin, 1995).

2.4. Phylogenetic analysis

For the SSU rDNA phylogeny 19 sequences belonging to microsporidia were retrieved from Genbank. The source of sequences selected for the analyses, included twelve closest matches in BLAST search and 6 outgroup taxa: (i) two *Amblyospora* species of the Clade 1 (*sensu* Vossbrinck and Debrunner-Vossbrinck, 2005); (ii) three taxa of "Marinosporidia" infecting marine and freshwater crustaceans, and (iii) *Bacillidium* and *Janacekia* representing another group of aquatic microsporidia (Clade 5, Vossbrinck and Debrunner-Vossbrinck, 2005). *Paramicrosporidium vanellae* from the super taxon Cryptomycota (James et al., 2013) (known also as Rozellomycota (Corsaro et al., 2014)), the closest fungi relative of Microsporidia (Corsaro et al., 2014), was used as a non-microsporidian outgroup. The sequences were aligned with Muscle (MEGA 5.05), with default parameters (Edgar, 2004). The final datasets resulted in 605 informative positions. Pairwise genetic distances were calculated by the Kimura-2 parameter method with a gamma distribution 1 (Tamura et al., 2011). The alignments were subjected to phylogenetic reconstructions by maximum likelihood (ML) using MEGA 5.05 (Tamura et al., 2011) and Bayesian inference using MrBayes 3.2 (Ronquist et al., 2012). ML phylogenetic analyses used GTR + G model of nucleotide substitution (Nei and Kumar, 2000) as suggested by Modeltest, with 1000 bootstrap replications. MrBayes was run for 1,000,000 generations and every 1000th generation was sampled. The first 25% of samples were discarded as burn-in, parameter values were summarized, and a consensus tree was constructed. Standard deviation of split frequencies, which estimates the precision of the clade probabilities, reached 0.007 after 1,000,000 generations.

3. Results

3.1. The microsporidium isolated from Cyclops sp.

3.1.1. Tissue tropism and light microscopy

The hypoderm and fat body of the singe infected copepod were loaded with mature spores (Fig. 1a), which substituted host tissues and were partly washed out during processing. Muscle and intestine were free from infection. On methanol-fixed smears only mature spores were identified. The spores measured 2.0 ± 0.04 × 3.6 ± 0.04 μm, ranging 1.7–2.3 × 3.1–4.0 μm (n = 20).

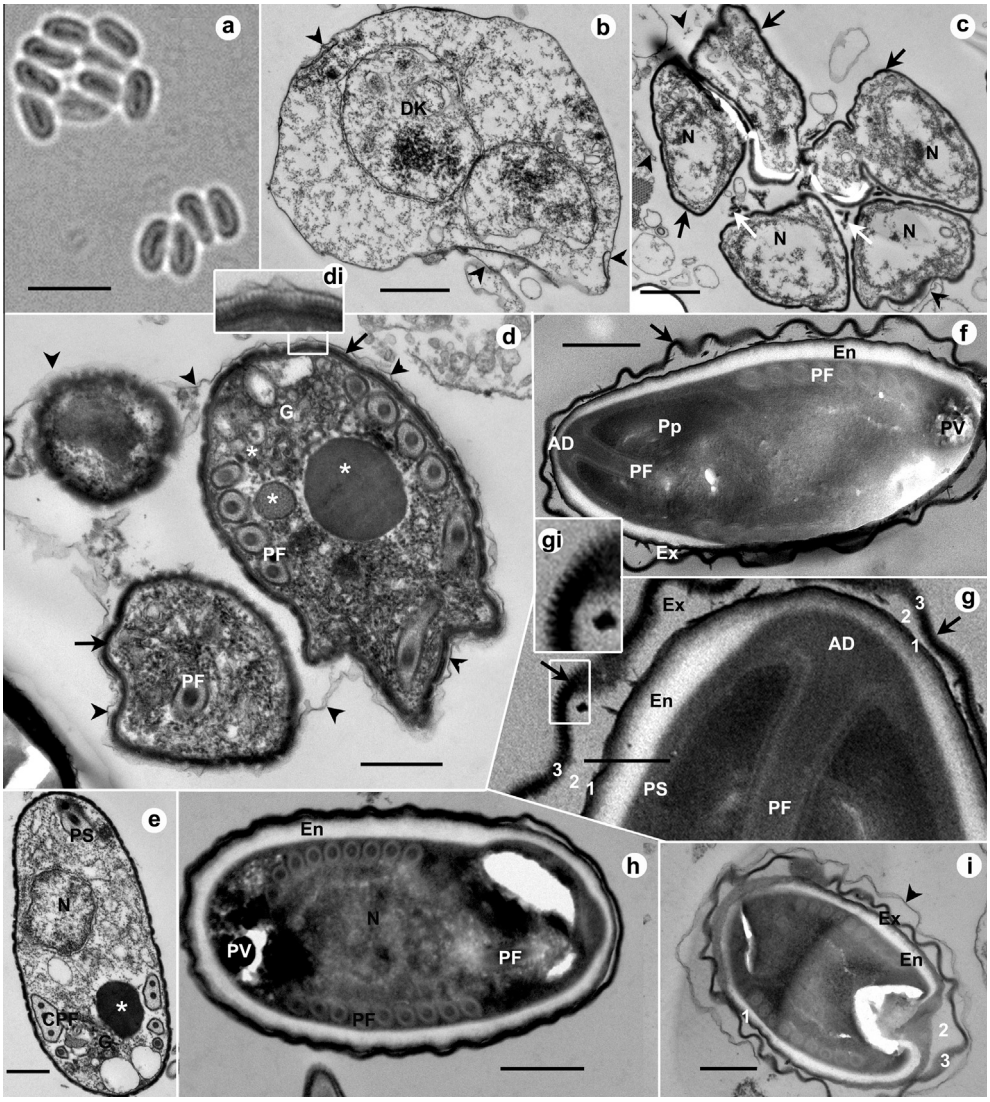

Fig. 1. *Alfvenia sibirica* sp. n. from *Cyclops* sp. (a) Light microscopy; (b-l) transmission electron microscopy. (a) Methanol-fixed unstained spores. (b) Meront-sporont transitional stage with the diplokaryon. In a few spots (arrowheads) an additional layer split off the plasma membrane. (c) A "rosette" of newly formed sporonts. Surrounding SV membrane (arrowheads) is poorly preserved. Excessive material of sporont envelopes within perisporontal space (lamellar-like secretion) is marked by white arrows, and sporont envelopes – by black arrows. (d) Three sporoblasts are enclosed in SV membrane (arrowheads). Their envelopes corresponding to the external layer of the exospore, are indicated by black arrows. Asterisks mark electron dense bodies associated with Golgi organelle, presumably containing polar tube proteins. (di) Enlarged portion of the sporoblast envelope (d) with the projections similar to those observed on the external layer of the exospore. (e) Sections through a sporoblast in the process of polar filament differentiation. Tubular-vesicular Golgi organelle, cisternae with polar filament precursors, polar filament coils and electron dense bodies (asterisk) are in the view. (f) A mature spore with the undulating external layer of the exospore (arrow). (g) A portion of the previous figure at higher magnification demonstrating the anchoring disk, polar sack, anterior straight region of the polar filament, and exospore composed of three layers (1, 2, 3), the external of which bears short projections. (gi) Short projections on the exospore surface at higher magnification. (h) A spore displaying nearly homogenous exospore, with hardly resolved three-layered structure. (i) A spore enclosed in two envelopes: SV membrane is indicated by arrowheads, undulating exospore – by arrows. Bars: a, 5 μm; b-c, 1 μm; d-f, h-i, 500 nm; g, 200 nm. AD, anchoring disk; CPF, cisterna with polar filament precursors; DK, nucleus in diplokaryotic arrangement; En, endospore; Ex, exospore; G, Golgi organelle; N, nucleus in monokaryotic arrangement; PF, polar filament; Pp, polaroplast; PS, polar sac; PV, posterior vacuole.

3.1.2. Electron microscopy

The earliest stage observed was a meront/sporont transitional stage, round to oval cells measured 3.2–3.8 × 5.0–5.3 μm. These cells contained a diplokaryon and were surrounded by an approximately 15 nm-thick membrane. In a few spots an additional 6–10 nm-thick layer split off the plasma membrane (Fig. 1b). Sporogonial plasmodia, the next developmental stage, were shapeless multinuclear cells (not shown). Nuclei migrated to the cell periphery prior to sporont division by rosette-like budding (Fig. 1c). The next stage observed on sections, were uninuclear sporoblasts sporadically covered with a thin (4–13 nm, averaged 8.9 ± 0.66 nm (n = 14)) membranous envelope of the sporophorous vesicle (SV) (Fig. 1d and e). Each SV enclosed up to 3 sporoblasts (Fig. 1d), but regularly one or two. Sporoblasts and young spores contained prominent electron dense bodies associated with polar filament precursors, and presumably composed of the polar tube protein (Fig. 1f and e). The remnants of these bodies transformed into posterior vacuole (posterosome) of mature spores, commonly poorly preserved. Sporoblast envelopes displayed layer of short and barely visible bristles on the surface (Fig. 1di). This "Brush-like" layer became more pronounced on the exospore of mature spores (Fig. 1gi).

Spores (Fig. 1f–i) measured 1.3 × 2.7 μm (1.0–1.4 × 2.6–2.9) on thin sections. Spore walls were 162.2 ± 4.78 nm thick (n = 19, range 132–195) and composed of the endospore 97.4 ± 5.49 nm (n = 10, range 67–121) and the exospore 79.7 ± 2.97 nm (n = 20, range

58–103) thick. The exospore consisted of two electron dense layers and a gap of low electron density separating these layers from each other. Two electron-dense layers were either attached to each other (Fig. 1h), or loosely arranged leaving electron lucid space in between (Fig. 1f, g and i). The external layer 32.6 ± 2.62 nm thick (n = 21, range 23–48) tended to detach from the spore surface and form an undulating sheet covering the spore. The outer surface of this sheet, like sporoblast envelopes, exhibited brush-like appearance due to projections measured 5–8 nm thick and in 14–46 nm long (Fig. 1g, gi). The anchoring disc was of a typical structure, with a polar sac embracing the anterior portion of the polaroplast. Polaroplast membranes were badly preserved and individual membranes were hardly visible (Fig. 1i–j). The anchoring disc formed a continuum with the uncoiled portion of the polar filament, which occupied about ¼ of the spore length (Fig. 1f and g). The isofilar polar filament displayed 8–10 coils of 97 nm in diameter in average (94–100 nm) arranged in one row (Fig. 1f, h–i). As a rule, the SV membrane disappeared by the time of spore maturation, but occasionally it was preserved. Spores then were enclosed in two undulating envelopes (Fig. 1i).

3.2. The microsporidium isolated from Daphnia magna

3.2.1. Tissue tropism and light microscopy

Unlike the above described species infection prevalence of this microsporidium in the examined pond exceeded 80%. Some of the infected water fleas exhibited external signs of pathology visible from the lakeshore: intensive (up to 10-fold normal body size) swelling and whitening of hypertrophied inner tissues visible through transparent teguments (Fig. 2a). Upon squeezing, cladocerans released sporophorous vesicles (SVs) enclosing 8–16, commonly 8–10 spores, and free spores (Fig. 2b and c). SV envelopes were relatively persistent. Spores liberated from SVs were surrounded by halos of amorphous material (Fig. 2b). Spores were pyriform, with one nucleus visible on methanol fixed Giemsa or DAPI-stained smears (not shown). Methanol-fixed spores (Fig. 2d) measured 2.3 ± 0.05 × 4.0 ± 0.06 μm; range 1.9–2.5 × 3.5–4.3 μm (n = 20). Hypoderm, underlying fat body and haemocytes were loaded with microsporidia spores (Fig. 2e). The presporal development was nearly completed by the time of sampling, and other than spore stages could be seen only in the samples prepared for electron microscopy. On thick sections stained with Methylene Blue, elongated meronts (2.0–2.5 × 3.0–6.0 μm) with 1–3 nuclei (Fig. 2f), roundish sporonts (2.8–4.2 × 3.7–4.9 μm) with a single large nucleus, and sporophorous vesicles (6.5–7.0 × 7.7–8.5 μm) with sporoblasts or mature spores were seen (Fig. 2g). The latter greatly dominated over all other stages.

3.2.2. Electron microscopy

The earliest stages observed were elongated cells with two to four, but commonly two nuclei. Nuclei in diplokaryotic association were never observed, however their arrangement suggested that they might have derived from recently dissociated counterparts of a diplokaryon (Fig. 3a). We term this stage "presporont" after previous authors reported this type of cells as a dominant stage in the prespore development of the microsporidium *Binucleata daphniae* (Refardt et al., 2008). Presporonts ranged from 3.2 to 7.0 μm in length and from 1.33 to 2.65 μm in width. Their cytoplasm looked dense due to numerous ribosomes and cisternae of endoplasmic reticulum scattered all over the cell (Fig. 3a and b). Presporonts divided to produce chains of irregularly shaped sporonts 1.9–2.3 μm in diameter (Fig. 3c). Sporonts underwent nuclear divisions and gave rise to multinucleate sporogonial plasmodia (Fig. 3d). Presporonts, sporonts and plasmodia were enclosed in additional envelope, a precursor of the sporophorous vesicle (SV) membrane (Fig. 3a–e). The next stage observed were SVs with sporoblasts at different steps of morphogenesis, surrounded by 10–13 nm thick membranous envelopes (Fig. 3e and f). The SVs were filled with finely granulated material of moderate electron density (Fig. 3e and f), and, occasionally, with 30–70 nm-thick multilayered lamellar-like structures sometimes seen on sections as round profiles (Fig. 3e and f), termed here as "lamellar secretion". Sections through these structures were composed of two electron dense layers separated by a transparent space and resembled the sections through sporoblast envelopes, the precursors of exospores (Fig. 3f). Likely, the pieces of lamellar secretion represented an excessive exospore material, released during sporoblast separation from the plasmodium via "rosette-like" division. Protrusions

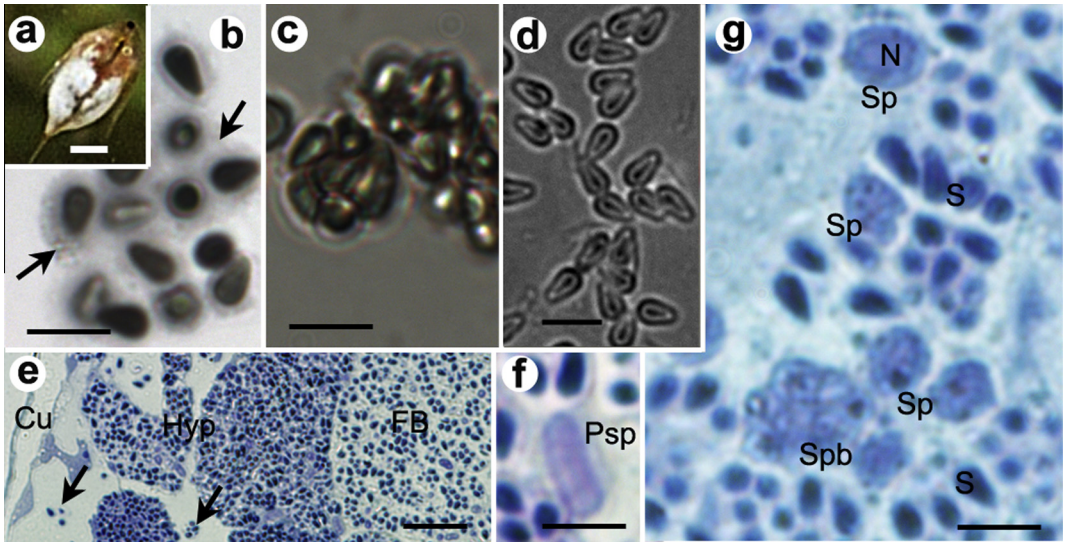

Fig. 2. Siberian isolate of *Agglomerata cladocera* from *Daphnia magna*, light microscopy. (a) Live water flea *Daphnia magna* with signs of microsporidiosis. (b and c) Spores liberated from glutaraldehyde-fixed crustaceans. (d) Methanlol-fixed unstained spores. (e–g) Thick section stained with Methylene Blue. (b) Individual spores are surrounded by halos of amorphous material. (c) Spores are aggregated in sporophorous vesicles (SVs) in groups of 8–10. (d) SVs disintegrate on methanol-fixed smears. (e) Section through cuticle (Cu), heavily infected hypoderm (Hyp) and fat body (FB). Arrows point to individual haemocytes loaded with spores. (f) Elongated "presporont" (Psp). (g) Section through infected tissue displaying spores (S); sporonts (Sp), and a sporophorous vesicle with sporoblasts (Spb). N, sporont nucleus. Bars: a, 1 mm; b-d; f-g, 5 μm; e, 20 μm.

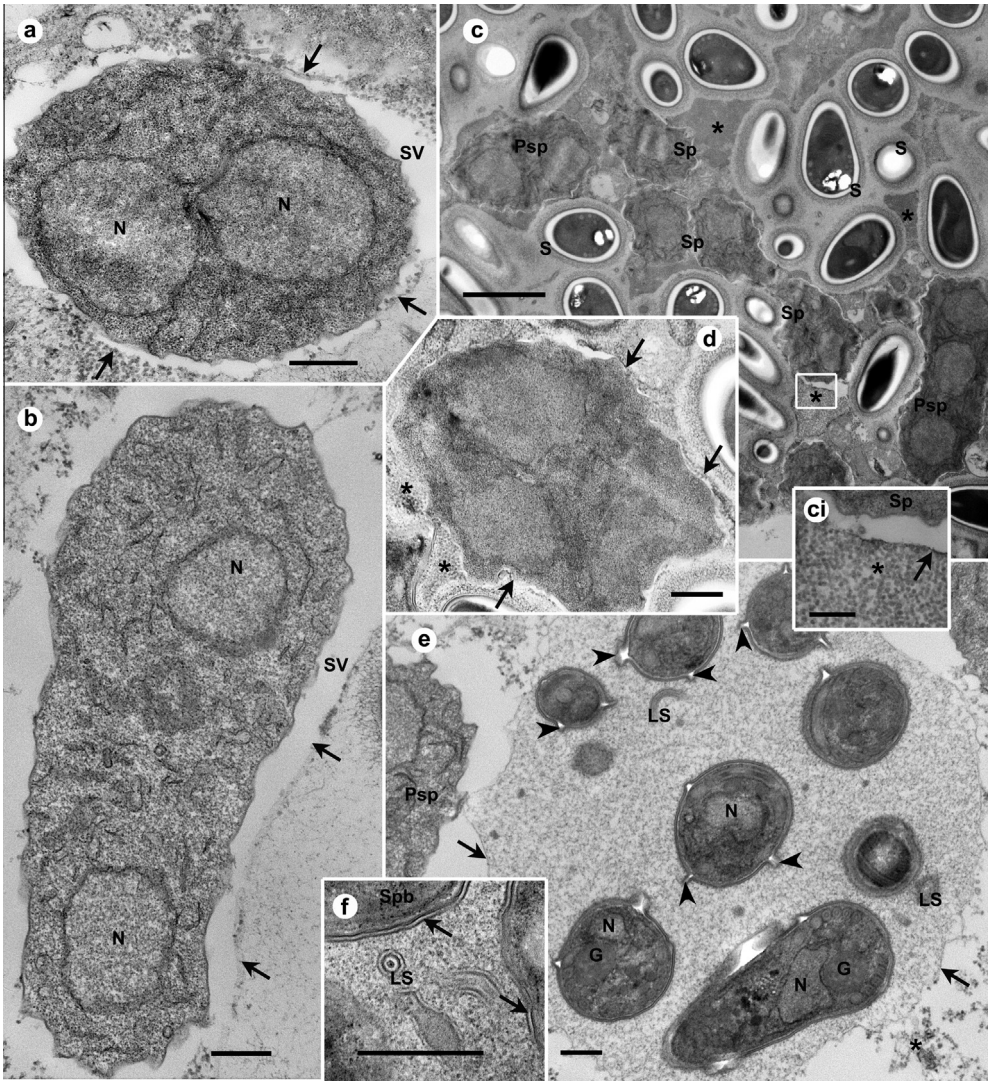

Fig. 3. Siberian isolate of *Agglomerata cladocera* from *Daphnia magna*: ultrastructure of prespore stages. (a) A section through a presporont enclosed in the sporophorous vesicle (SV). Arrangement of two nuclei suggests they might have derived from dissociated counterparts of a diplokaryon. Arrows indicate sporophorous vesicle (SV) membrane. (b) A typical elongated presporont with two nuclei and short cisternae of endoplasmic reticulum scattered all over the cytoplasm. Arrows indicate SV boundaries. (c) SVs enclosing mature spores, two presporonts, and a chain of irregularly shaped unicellular sporonts, the products of presporont division. Asterisks mark granular-tubular secretion abundant around sporonts sporogonial plasmodia. (ci) A portion of granular-tubular secretion adjacent to SV membrane (arrow), at higher magnification. (d) A section through multinucleate plasmodium enclosed in SV membrane (arrows). Asterisks mark granular-tubular secretion. (e) SV filled with finely granulated material of moderate electron density, contain sporoblasts. Inclusions of lamellar-like secretion (LS), the excessive exospore material resulted from sporoblasts segregation. The sites of emerging of this material on the sporoblast surfaces are indicated by arrowheads. Arrows point to SV membrane. Asterisks mark granular secretion associated with SV surface. Bars, a-b, d-f, 500 nm; c, 2 μm; ci, 250 nm. G, Golgi-derived granules containing polar tube proteins; LS, lamellar secrete; Mi, mitochondria; N, nucleus; PF, polar filament; Psp, presporont; Sp, sporont (sporont mother cell); Spb, sporoblast; SV, sporophorous vesicle.

composed of folded exospore-type material, were frequently seen on the surfaces of sporoblasts and young spores (Fig. 3e).

SEM images demonstrated the surface of SVs was covered with irregularly arranged tubules and blebs (Fig. 4a) corresponding probably to granular-tubular secretion derived from denser secretion observed around sporonts (Fig. 3ci) and occasionally seen in host cytoplasm in vicinity of SVs (Fig. 3e).

Protrusions on the spore surfaces and lamellar secretion in SV lumens disappeared upon spore maturation (Fig. 4b). Finely granulated material transformed into a network of 6–10 nm thick fibrils concentrated around spores, and was hardly distinguishable from the "episporal threads" projected from the spore surface, and sometimes connected the exospore with the SV membrane (Fig. 4c and d).

Spores (Fig. 4a–e) on transverse sections measured 1.2–1.5 μm wide (in the broadest part) and 2.1–2.6 μm long. They were pyriform with pointed anterior ends, and slightly elongated single nucleus located centrally, a bit closer to the posterior pole (Fig. 4c and e). The spore wall was about 150–170 nm thick, except for 80 nm-thick anterior region. The wall was composed of a 21–26 nm wide multilayered exospore, translucent endospore and plasma membrane. The exospore layers included: an electron-dense external 5–6 nm thick layer, translucent median layer of about twice that thick, and internal electron-dense layer 6–8 nm thick. The latter was associated with diffuse amorphous transitional layer of intermediate electron density located at the border of exospore and endospore (Fig. 4di). The episporal coat was built of 6–12 nm-wide threads extended 100–300 nm outwards (Fig. 4d, di). This layer likely corresponded to halos observed around spores in light microscope and presumably contributed to the increase of the spore buoyant density (Fig. 2b). Polar filament was slightly "anisofilar" or "heterofilar" according terminology of Voronin (1989), with one or rarely two anterior coils slightly differentiating from other 4–5 coils by size (111–142 nm vs. 72–105 nm)

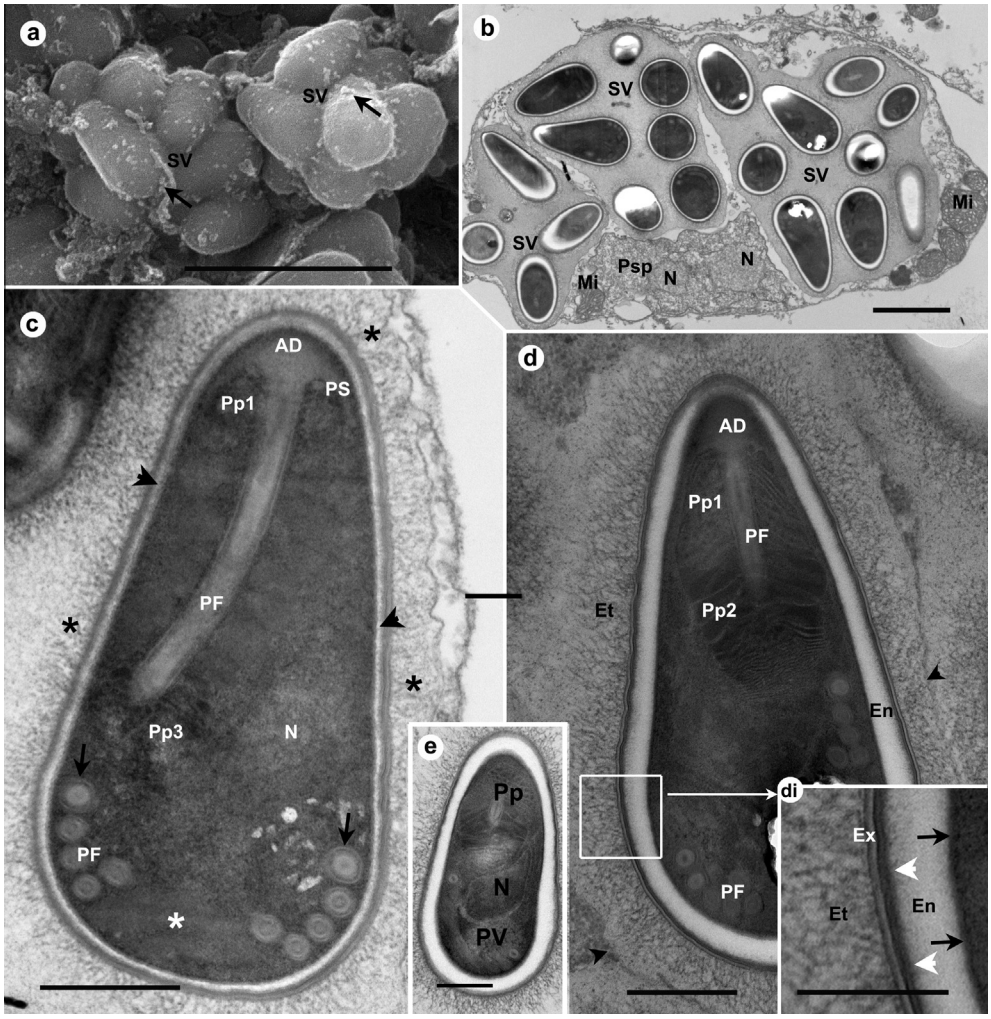

Fig. 4. Siberian isolate of *Aglomerata cladocera* from *Daphnia magna*: ultrastructure of spores. (a) A sporophorous vesicle (SV) with mature spores, SEM. Arrows point to blebs and tubules on SV surface corresponding to granular-tubular secretion associated with the surface of SVs, observed on sections. (b) A section through a host cell (presumably a haemocyte) containing SVs with mature spores and a two-nucleate presporont. No host organelles are seen, except mitochondria. (c) A young spore with a thin endospore (arrowhead) and typical organelles resides in a sporophorous vesicle filled with fine granular-tubular secrete concentrated around spore surface (asterisks). Arrows point to the anterior polar filament coils, which are larger and exhibit slightly different internal structure comparatively with the ones located posteriorly. The most distal part of polaroplast (Pp3) is composed of tubules. (d, di) A spore with a well-developed envelope composed of the plasma membrane (di, arrows), thick endospore, amorphous transitional layer (white arrowheads), 3-layered exospore, and episporal coat of 6–12 nm projections extended outwards, occasionally contacting the SV membrane (black arrowheads). (e) A spore with elongated nucleus (N) and well preserved posterosome (posterior vacuole) filled with membranous material. Bar, a, 5 μm; b, 2 μm; c-e, 500 nm; di, 250 nm. AD, anchoring disk; En, endospore; Ex, exospore; Mi, mitochondria; N, nucleus; PF, polar filament; ET, episporal tubules; Pp1, Pp2, Pp3, parts of polaroplast; PS, polar sac; Psp, presporont; PV, posterior vacuole; S, mature spores; SV, sporophorous vesicles.

and structure (Fig. 4c). The uncoiled part of the polar filament was 1.0–1.4 nm long (up to two thirds of the spore length). It turned to the side of the spore on longitudinal sections and nearly touched the spore wall. The final coiled section of the polar filament was composed of 5–6 coils, arranged regularly in one row. The second row, if present, included one coil (Fig. 4c). Posterior vacuole (posterosome) was composed of membranous material (Fig. 4e). In most spores due to high lipid concentration the posterosome was crushed out during processing and seen as "holes" on sections. Polaroplast was tripartite, composed of the anterior portion of wide anastomosing chambers, the intermediate region of tightly packed lamellae, and the distal part built of tubules branching from the very posterior end of the uncoiled region of the polar filament (Fig. 4c and d).

3.3. SSU rDNA-based phylogenetic analyses

The sequences obtained from the *Cyclops* and *Daphnia* microsporidia were 862 and 857 base pairs long, with 56% and 52% GC content (Table 1); they were deposited in GenBank under accession numbers KT950766 and KT950767 respectively. Alignment of 652 informative positions of twenty sequences analyzed by Bayesian and Maximum Likelihood phylogenetic algorithms, produced identical tree topology, overall concurrent with previously published phylogenies (Stentiford and Dunn, 2014; Vossbrinck et al., 2004; Vossbrinck and Debrunner-Vossbrinck, 2005). The analyzed taxa were distributed among three superclades, defined by previous authors as "Clade I" and "Clade V", microsporidia of freshwater origin, and "Clade IV", microsporidia of terrestrial origin (Vossbrinck and Debrunner-Vossbrinck, 2005; Vossbrinck et al., 2014). Both novel sequences belonged to the so-called "Aquatic outgroup" (Vossbrinck et al., 2004) (AOG), a sister group to the *Amblyospora-Andreanna* branch within the Clade I. The latter clustered with Clade IV, which was represented in our dataset by marine and freshwater dwelling microsporidia, *Paranucleospora theridion*, *Mrazekia macrocyclopis*, and *Agmasoma penaei*. The *Bacillidium-Janacekia* lineage representing Clade V branched independently (Fig. 5).

Table 1
SSUrDNA GC content and pairwise evolutionary distances[a] among microsporidia belonging to the Aquatic outgroup.

		GC%	1	2	3	4	5	6	7	8	9	10	11	12
1	*Alfvenia sibirica* sp. n.	56	–	84.91	87.58	84.13	83.04	82.84	89.58	87.22	84.96	82.70	85.53	82.09
2	*Agglomerata cladocera* (Si[b])	52	0.15	–	91.68	**99.07**	87.20	87.01	87.02	91.16	88.15	84.03	**97.66**	80.39
3	*Berwaldia schaefernai*	55	0.12	0.08	–	90.62	91.17	91.00	90.12	**99.07**	90.26	85.20	92.03	81.60
4	*Binucleata daphniae*	52	0.16	**0.01**	0.09	–	86.06	85.86	86.26	90.27	87.41	82.84	**97.02**	79.57
5	*Gurleya daphniae*	51	0.17	0.13	0.09	0.14	–	**99.85**	84.95	90.47	85.73	80.98	87.17	75.69
6	*Gurleya vavrai*	51	0.17	0.13	0.09	0.14	**0.00**	–	84.76	90.29	85.54	80.77	86.98	75.46
7	*Hazardia milleri*	59	0.10	0.13	0.10	0.14	0.15	0.15	–	89.59	90.07	87.43	88.13	85.78
8	*Larssonia obtusa*	55	0.13	0.09	**0.01**	0.10	0.10	0.10	0.10	–	89.72	84.63	91.69	81.00
9	*Marssoniella elegans*	54	0.15	0.12	0.10	0.13	0.14	0.14	0.10	0.10	–	85.30	87.94	81.48
10	*Octosporea muscadomestticae*	57	0.17	0.16	0.15	0.17	0.19	0.19	0.13	0.15	0.15	–	83.85	78.34
11	*Senoma globulifera*	53	0.14	**0.02**	0.08	**0.03**	0.13	0.13	0.12	0.08	0.12	0.16	–	81.17
12	*Trichotuzetia guttata*	58	0.18	0.20	0.18	0.20	0.24	0.25	0.14	0.19	0.19	0.22	0.19	–

[a] Distance matrix was calculated by Kimura-2-Parameter analysis basing on 652 informative positions of SSUrDNA sequence. Lower diagonal, distance matrix; upper diagonal, % similarity = [(1 − distance value) × 100]%. The lowest (<0.04) values of the distance and the highest (>96%) values of the similarity are marked by bold font.
[b] Si, Siberian isolate.

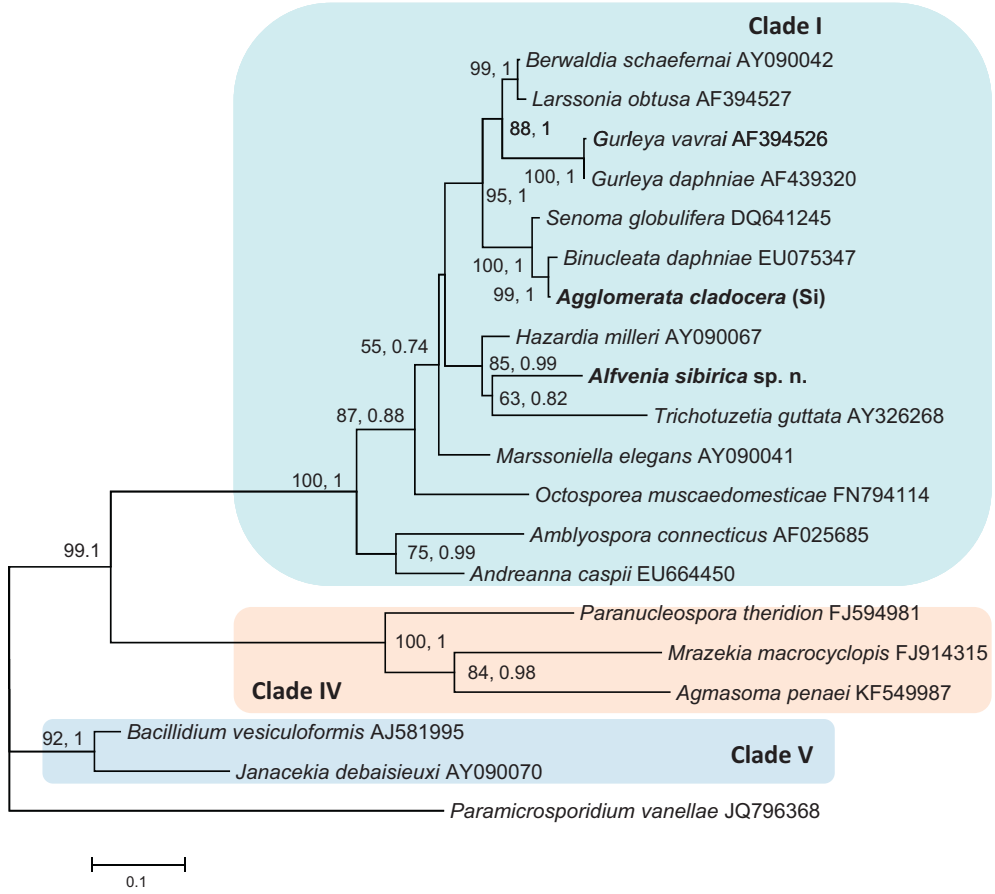

Fig. 5. The ssrDNA-inferred phylogenetic tree produced by Maximum Likelihood (ML) and Bayesian (Mr.Bayes) algorithms. The analyses were based on alignment of 19 microsporidian sequences and 652 informative positions. *Paramicrosporidium vanellae* was the source of the outgroup sequence. The analyzed taxa were distributed among three super clades: "Clade I", "Clade 5", and "Clade IV" of microsporidia of terrestrial origin (Vossbrinck, Debruner-Vossbrinck, 2005). The species names are followed by GenBank accession numbers. The novel sequences are printed in bold. Si, Siberian isolate. ML bootstrap values are shown first, followed by Mr.Bayes posterior probabilities. Node supports <55/0.70 (ML/Mr.Bayes) are not shown. Scale bar corresponds to 0.1 substitutions per site.

The values of pairwise distances/similarities calculated by Kimura-2 P analysis between the microsporidium from *Cyclops* sp. and any other representative of the Aquatic outgroup varied from 0.1042/89.58% (*Hazardia milleri*) to 0.1791/82.09% (*Trichotuzatia guttata*). The same parameter for *Daphnia* microsporidium altered from 0.0093/99.07% (*B. daphniae*) and 0.0234/97.66% (*Senoma globulifera*) to 0.1961/80.39% (*T. guttata*) (Table 1).

4. Discussion and taxonomic considerations

4.1. Microsporidium from Cyclops sp. is a new species of the genus Alfvenia

The novel microsporidium isolated from *Cyclops* sp. resembled the previously described species of the genus *Alfvenia* (Larsson, 1983; Vidtmann and Sokolova, 1995) by numerous morphological

and developmental characters summarized in Table 2. Morphological characters of this microsporidium corresponded to the diagnosis of this genus: "Sporont diplokaryotic; sporogonial plasmodium divides into small number of sporoblasts. Spores are oval. Polar filament isofilar. Sporoblasts with a thick multilayered exospore. Sporophorous vesicle devoid tubules" (Larsson, 1983). In addition, tendency of the exospore splitting, similar exospore width and exospore/endospore ratio (Fig. 8c, Larsson, 1983), as well as brush like appearance of the exospore visible though only in immature spores (Fig. 8a, Larsson, 1983), are characteristic for the type species *Alfvenia nuda*. Hence the described species was assigned to the genus *Alfvenia*. It can be easily differentiated from other two species of the genus described so far, *A. nuda* Larsson, 1983 and *Alfvenia ceriodaphniae* Vidtmann and Sokolova, 1995. The Siberian microsporidium can be differentiated from *A. ceriodaphniae* by parasitizing a copepod, but not a cladoceran host, the smaller size, and arrangement of polar tube filaments strictly in one row (Table 1). Though the novel species reminds the type species *A. nuda* by the size and related host species, it has a shorter polar tube (8–10 coils versus 12–14 in *A. nuda*), which is always arranged in one row, whereas in *A. nuda* "filament coils are irregularly arranged" (Larsson, 1983). Also, the number of spores within a sporophorous vesicle reordered for *A. nuda* never exceeded 2 (Larsson, 1983), while in the case of the Siberian microsporidium, three spores per one SV was not unusual. *A. nuda* is also characterized by more persistent SV membrane. In addition split of the exospore and detaching of the external exospore layer observed in *A. ceriodaphniae* and in the novel species, was not mentioned in description of *A. nuda* (Larsson, 1983). The above mentioned differences allow us to describe this microsporidium as a new species of the genus *Alfvenia*, *A. sibirica* sp. n.

Taxonomic summary

***Alfvenia sibirica* sp. n**. Sokolova, Senderskiy and Tokarev.

Host and locality: unidentified *Cyclops* sp., from the lake Krotova Lyaga, Karasuk District, Novosibirsk region, South-Western Siberia, Russia (56°32′N, 29°31′E).

Tissue tropism: hypodermis and fat body.

Meronts not described.

Sporonts diplokaryotic round to oval in shape.

Sporogonial plasmodia multinucleate, divide by rosette-like budding. The membrane of the sporophorous vesicle (SV) is 4–13 μm thick, derives from the external layer of the sporont or sporogonial plasmodium envelope. SV membrane may adhere to the plasmodium. No tubules derive from the surface of the sporogonial plasmodia or daughter sporoblasts, and none occur inside the SV lumen.

Spores are oval, measured 2.0 ± 0.04 × 3.6 ± 0.05 (1.7–2.3 × 3.1–4.0) μm (n = 20) (methanol-fixed). Sporophorous vesicle membrane (SVM) is thin and subpersistent, and most mature spores lay free in host tissues, whereas sporoblasts and immature spores occasionally lay within SVM individually or in groups of two or three. The anchoring disc is of a typical structure with a polar sac embracing the anterior portion of the polaroplast. The uncoiled portion of the isofilar polar filament occupies about ¼ of the spore length. The polar filament displays 8–10 coils arranged in one row. Polaroplast is bipartite, with the anterior membranes packed tighter than the posterior ones. The exospore is about 80 nm thick, and consists of at least 3 layers: internal layer of low electron density, and two denser layers. In mature spores the very external exospore layer about 30 nm thick, tends to detach from the surface and form an undulating sheet covering the spore surface. The outer surface of this sheet exhibited "brush-like appearance" due to projections in average 6 nm wide (range: 5–8 nm) and 30 nm (range 14–46 nm) long.

Etymology. The species name refers to the region of sampling.

Type material. Slides with methanol smears of infected *Cyclops* sp. are deposited in the microsporidia collection of the Institute of Plant Protection, St. Petersburg, Russia (Prof. Issi's collection). Slides with semi-thin sections, embeddings, grids with thin sections, and images of thin sections, labeled "YT-3_Cyclops1" are stored in the collection of the first author.

4.2. Microsporidium from Daphnia magna and overview of Agglomerata spp.

Morphological and developmental traits of the microsporidium isolated from Siberian population of *D. magna*, do not allow its distinguishing from *A. cladocera* isolated from the same host species in England (Larsson et al., 1996). The comparison of morphological character of two isolates is summarized in Table 3. Indeed, ultrastructural analysis suggests the microsporidium isolated from *D. magna* in Siberia is *A. cladocera* (Table 3). Slight variations in measurements, as well as different arrangement of polar filament coils – in one row in English isolate versus occasionally in two rows in Sibirian isolate, may be attributed to variations among geographical populations. Therefore we suggest to refer to the novel isolate as "*Agglomerata cladocera* (Sibirian isolate)" (*A. cladocera* (Si)).

Table 2
Characters of *Alfvenia* spp.

Characters	*Alfvenia nuda* (Larsson, 1983)	*Alfvenia ceriodaphniae* (Vidtmann, Sokolova, 1985)	*Alfvenia sibirica* (herein)
Host	*Acanthocyclops vernalis* (Maxillopoda, Cyclopidae)	*Ceriodaphnia eticulata* (Branchiopoda, Daphniiidae)	*Cyclops* sp. (Copepoda) (Maxillopoda, Cyclopidae)
Locality	Sweden	Lithuania	W. Siberia
Tissue tropism	Adipose tissue, hypodermis	Hypodermis	Adipose tissue, hypodermis
Sporont, nucleus	DK	DK	DK
Sporogonial plasmodium: nuclei, division type	Individual nuclei; rosette-like budding	Individual nuclei; rosette-like budding	Individual nuclei; rosette-like budding
Sporophorous vesicle membrane: origin; structure; connection with the exospore	Derives from sporont envelope; thin sub-persistent; adhere to exospore	Derives from sporoblast envelope; thin subpersistent; adhere to exospore	Derives from sporont envelope; thin sub-persistent; adhere to exospore
Sporophorous vesicle: number of spores; tubular secretion	1–2 spores; no tubular secret	1 spore; no tubular secret	1–3 spores; no tubular secret
Spore size (μm): live; fixed	3.5–3.9 × 2.5–2.8; 2.5–3.0 × 1.5–1.8	4.2–4.8 × 2.9–3.5	3 × 1.5
Spore shape	Oval, with pointed apical end	Oval, egg shaped	Oval
Exospore	Multilayered; smooth (no filaments); undulating	3-layered; smooth (no filaments); undulating	3-layered; smooth (no filaments); undulating
Spore, nucleus	1N	1N	1N
Polar filament	Isofilar; 12–14 coils in 1–2 rows	Isofilar; 8–9 coils in 1–2 rows	Isofilar; 8–10 coils in 1 row
Polaroplast	Bipartite: lamellar-lamellar	Bipartite: lamellar-chamber	Bipartite: lamellar-lamellar

Table 3
Comparison of two isolates of *Agglomerata cladocera*.

Characters	*A. cladocera* (Larsson et al., 1996)	*A. cladocera* (Siberian isolate) (herein)
Host	*Daphnia magna*	*Daphnia magna*
Locality	W. Siberia	England
Tissue tropism	Hypoderm	Hypoderm, haemocytes, fat body
Presporont	Elongated merogonial plasmodium with 1–3 nuclei	Elongated merogonial plasmodium with 1–3 nuclei
Sporogonial plasmodium: nuclei; division type	Individual nuclei; rosette-like	Individual nuclei; rosette-like
Sporophorous vesicle membrane: origin; structure; connection with the exospore	From meront envelope; 5 nm thick, persistent; 5 nm thick fibrils fill SV and connect SVM with exospore at early stage of sporogenesis	From meront envelope; 11–13 nm thick, persistent; 5–6 nm thick fibrils fill SV, may connect SVM with exospore at early stage of sporogenesis
Sporophorous vesicle: number of spores; type of inclusions; shape; size (μm)	10–16 (>8) spores; 5–9 nm fibrils, 43–117 nm lamellar-like inclusions; oval; 4 × 7	8–16 spores; 6–10 nm fibrils, 30–70 nm lamellar-like inclusions, patches of amorphous dense material; oval; 5.9–7.8 × 6.7–8.9
Spore size (μm)	1.5–2.2 × 3.0–4.5 (live); 1.6–2.1 × 2.7–3.4 (fixed)	1.9–2.6 × 3.5–4.2 (GA fixed)
Spore shape	Pyriform, pointed anterior pole	Pyriform, pointed anterior pole
Spore envelope	159–165 nm	150–170 nm
Exospore	24 nm; 3 layered (5 + 11 + 8); exospore/endospore intermediate layer; not undulating, solid	21–26 μm; 3 layered (5–6 + 10–12 + 6–8) μm; exospore/endospore inter-mediate layer; not undulating, solid
Episporal structures	5–6 nm thick fibrils extending 327 nm outwards	6–12 nm thick fibrils extending 100–300 nm outwards
Spore nucleus	Single, located posteriorly	Single, located posteriorly
Polar filament: type; No of anterior + posterior coils (diameter, nm)	Slightly anisofilar; 1–2 (84–117 nm) + 3–4 (55–79), uncoiled part 2/3 of spore length	Slightly anisofilar: 1–2 (111–142) + 4–5 (72–105); uncoiled part up to 2/3 of spore length
Polaroplast	Tripartite: chamber + lamellar + tubular	Tripartite: chamber + lamellar + tubular

Up today seven *Agglomerata* spp. have been recorded: *A. sidae*, the type species (Larsson and Yan, 1988), *A. cladocera* (Larsson et al., 1996), *Agglomerata volgensae* (Larsson and Voronin, 2000), *Agglomerata connexa* (Ovcharenko and Wita, 2001), *Agglomerata bosminae* (Voronin, 1986, 1990), *Agglomerata simocephali* (Voronin, 1986) and *Agglomerata lacrima* (Bronnvall and Larsson, 2001). All these species infect cladocerans, except *A. lacrima*, a parasite of a copepod *Acanthocyclops vernalis*. Four *Agglomerata* spp. were studied with electron microscopy. Ultrastructural features of all *Agglomerata* spp. are fairly consistent (Table 4). The apomorphic character of *Agglomerata* spp. is the presence of 5–12 nm wide fibrils connecting exospore of sporoblasts or spores with SVM. These fibrils might conspicuously persist in mature spores holding them together in polysporous SVs, like in *A. sidae* (Larsson and Yan, 1988), *A. bosminae* (Voronin, 1986, 1990) and *A. simocephali* (Voronin, personal communication), or be less noticeable like in *A. connexa* (Ovcharenko and Wita, 2001) and *A. volgensae* (Larsson and Voronin, 2000). The fibrils may disappear upon spore maturation but remain as a coat of brush-like protuberances on the exospore like in *A. cladocera*, or present only at the early sporoblast stage, gradually vanishing afterwards and leaving no traces on the exospore of mature spores, like in *A. lacrima* (Bronnvall and Larsson, 2001).

4.3. Phylogenetic relationships within Aquatic outgroup (AOG)

Within AOG, SSU rDNA phylogenetic analysis identifies two major well supported branches (Fig. 6): the *Alfvenia-Trichotuzetia-Hazardia* and *Agglomerata-Binucleata-Gurleya-Senoma-Larssonia-Berwaldia* lineages. Interestingly, the members of the former group parasitize predominantly cyclopids (Maxillopoda, Copepoda) (*Cyclops* sp. icon, Fig. 6), whether the representatives of the latter are mainly associated with cladocerans (Brachiopoda, Cladocera) (*Daphnia* sp. icon, Fig. 6). AOG clade also includes a few taxa with dipteran hosts (*Chironomus* sp. icon) which likely suggest that the common ancestors of amblyosporids and AOG possessed polyxenous life cycles involving a dipteran and a copepod host, as *Amblyospora connecticus* and other extant amblyosporids (Vossbrinck et al., 1998). On the phylogenetic tree, *A. sibirica* clustered with *T. guttata* (Figs. 5 and 6). However, rather low statistical support for this branch, as well as high value of phylogenetic distance between *A. sibirica* and *T. guttata* (Table 1) leave the relations between these two taxa unresolved until more taxa and/or genes are available for the analysis. The *Alfvenia-Trichotuzetia* branch appeared as a sister lineage to *H. milleri*, a mosquito microsporidium, and this grouping was relatively well supported (Figs. 5 and 6). *H. milleri* was also the closest taxon to *A. sibirica* in K2P distance analysis.

A. cladocera fell into another lineage of AOG, clustered with *B. daphniae* and displayed as high as 99.07% of genetic similarity to this species in pairwise distance analysis, as well as identical GC content (52%) (Figs. 5 and 6, Table 1). In fact, alignment of 840 bp-long *A. cladocera* sequence against the *B. daphniae* orthologue demonstrated extremely high homology of two sequences: among only nine single nucleotide polymorphisms, eight were transitions (C-T), and only one – a transversion (G-T, position 360) (Fig. S1). Taking in account also very high structural similarity of *B. daphniae* and *A. cladocera* (Table 4), and the same host species, such relatedness of SSU rDNA sequence would suggest that *A. cladocera* and *B. daphniae* are rather the congeners, and the genus *Binucleata* should be treated as a junior synonym of *Agglomerata*. However, similarly low pairwise distance (0.009) was observed between *Berwaldia schaefernai* and *Larssonia obtusa*, the species with fairly contrasting morphology (Vávra and Larsson, 1994; Vidtmann and Sokolova, 1994). For comparison, congeners *Gurleya daphniae* and *Gurleya vavrai* exhibited lower genetic distances (0.0015). Though morphologically *B. daphniae* and *Agglomerata* spp. are similar in many ways, *B. daphniae* is lacking two important characteristic features of *Agglomerata* spp.: (i) fibrils connecting the exospore with the membrane of sporophorous vesicle (SVM), and (ii) multilayered exospore, with at least 3 layers of alternate electron density (Table 4). The exospore of *B. daphniae* is, on the contrary, uniform and smooth (Refardt et al., 2008). Hence, minor but salient morphological differences prevent us from abolishing the monotypic genus *Binucleata* until more *Binucleata* species are available for ultrastructural and phylogenetic analyses.

The *Agglomerata-Binucleata* dichotomy clustered with *S. globulifera* (Fig. 6). *S. globulifera* displayed similar GC content (53%) and low values of genetic distance to *B. daphniae* (0.0298) and *A. cladocera* (0.0234) (Table 4). Given *S. globulifera* is quite different morphologically and parasitizes a dipteran host (Simakova et al., 2005), we presume that this species (similar to *H. milleri* in the

Table 4
Morphological and ultrastructural characters of *Agglomerata* spp. and *Binucleata daphniae*.

Characters	*A. sidae* (Larsson, Yan, 1988)	*A. cladocera* (Larsson et al., 1996; herein)	*A. volgensae* (Larsson, Voronin, 2000)	*A. connexa* (Ovcharenko, Wita, 2000)	*A. lacrima* (Bronnvall, Larsson, 2001)	*Binucleata daphniae* (Refardt et al., 2008
Host genus	*Holopedium*	*Daphnia*	*Daphnia*	*Daphnia*	*Acanthocyclops*	*Daphnia*
Tissue[a]	Hyp; adip; haem	Hyp; adip; haem	Hyp; adip	Adip	Hyp; adip	Hyp
Presporont, nuclei no.[b]	2, 3, 4 N	1, **2**, 3 N	1 N	No data	1 N	**2** N
Sporogonial plasmodium division	Rosette-like	Rosette-like	Rosette-like	Rosette-like	Rosette-like	Rosette-like
SVM: structure; origin	Persistent; from sporont envelope	Persistent, 12 nm; from meporont envelope	Fragile, 5 nm; from sporont envelope	Fragile; from sporont envelope	Fragile; from sporont envelope	Fragile, 12 nm; from meporont envelope
SVM-exospore link	Fibrils	Fibrils	Fibrils	Fibrils	Fibrils	None
SV inclusions[c]	Thread-like, LS	Thread-like, LS	Thread-like, LS	Thread-like, LS	Thread-like, LS	Thread-, granular-like
SV, no. of spores[b]	8, **16**, 32, >32	8, >8–16	1 or 4, **8**, 16	**1**, 2, 4, 8	4, 6, **8**, 12	**8**, 16
Spore size: live; fixed, μm	1.5–2.0 × 2.5–3.0	1.5–2.2 × 3.0–4.5; 1.6–2.1 × 2.7–3.4	1.7–2.0 × 3.1–2.0; 1.9–2.2 × 3.0–3.4	2.7 × 4.0; 2.0 × 3.4	2.6 × 4.4; 1.6 × 3.7	2.3–2.7 × 4.5 – 5.3; 2.2 × 3.9
Spore shape	Pyriform	Pyriform	Pyriform	Pyriform	Pyriform	Pyriform
Spore wall width (nm)	123–179	150–170	185	150–160	140–150	130
Exospore width (nm); number of layers	30; 5	23–26; 3	38; 7	No data; 3	35–39; 4	30; 1
Episporal structures; width × length (nm)	Tubules; no data	Fibrils; 5–6 × 100–300	Fibrils; 6 × 30	Fibrils; No data	Fibrils; 10 × 15 in immature spores	None
Polar filament type; numbers of anterior + posterior coils (diameter, nm)	Heterofilar; 1–3 (120–142) +3–4 (96–106)	Heterofilar; 1–2 (100) + 1–2 (80)	Heterofilar; 2–3 (92) + 2–3 (73)	Isofilar; 6–7 (140)	Heterofilar; 1–2 (135–140) + 4 (105–110)	Heterofilar; 3–5 (200) + 3–5 (130)
Polaroplast[d]	L + L + T	L + L + T	L + L	L + L + T	L + L + T	L + L

[a] Tissue types: hyp, hypoderm; adip, adipocytes; haem, hemolymph.
[b] No, number of nuclei or spores: the dominant no. is bolded.
[c] SV inclusions: thread-like, composed of thread- like fibrils 7–15 nm in diameter.
[d] Polarplast regions: L, lamellar, T, tubular. Other abbreviations: LS – lamellar secretion; N – nucleus; SV – sporophorous vesicle; SVM – SV membrane.

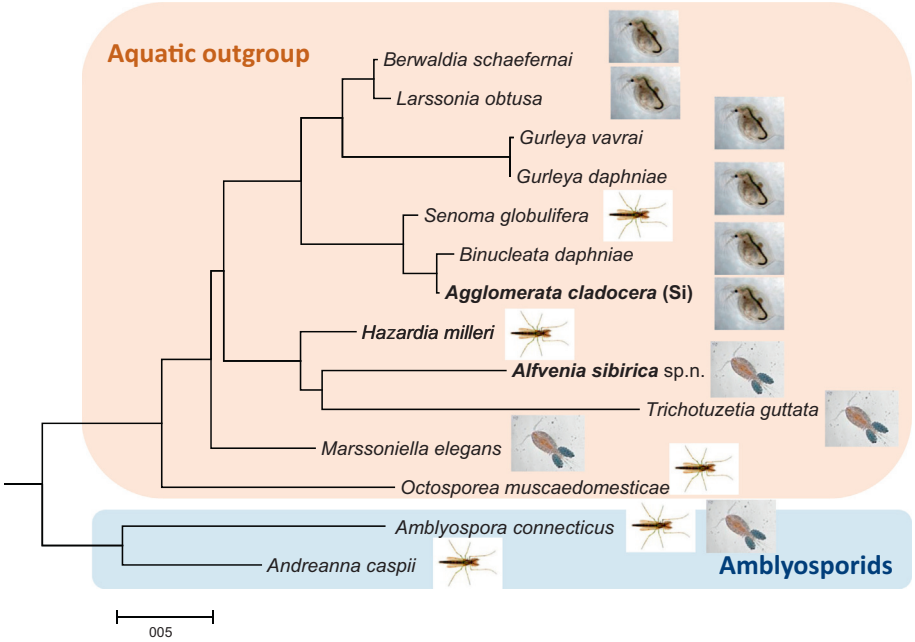

Fig. 6. The subtree of the tree depicted in Fig. 5. Both novel sequences (in bold) fell into "Aquatic outgroup" (AOG). Two major branches can be identified within AOG. The members of the first *Alfvenia-Trichotuzetia-Hazardia* lineage parasitize cyclopids (*Cyclops* sp. icon), with the exception of *Hazardia milleri* infecting mosquito hosts (*Chironomus* sp. icon). The representatives of the *Agglomerata-Binucleata-Gurleya-Larssonia-Berwaldia* lineage are mainly associated with cladocerans (Brachiopoda, Cladocera), with the exception of *Senoma globulifera* parasitizing dipterans. Scale bar corresponds to 0.05 substitution per site.

Afvenia-Hazardia lineage) exemplify an evolutionary descendant of the "mosquito morph" of the ancestral dixenous microsporidium. It cannot be excluded that some extant AOG representatives may require an alternate host as well, which has not been yet discovered (Refardt et al., 2008).

Evolutionary successors of a "copepod morph" of the common ancestor have probably diversified as parasites of microcrustaceans. Whether switch to cyclopids have occurred from a cladoceran or dipteran host cannot be concluded from the presented analysis, mainly because of the lack of sequence data on most AOG members. Interestingly, cyclopids and daphniids share similar habitat, but they are quite different in oxygen consumption, nitrogen and phosphorous content, and other biochemical characters (Arhonditsis and Brett, 2005; Bertilsson et al., 1995). They also exhibit different temperature limitations: copepods have wider temperature tolerance range, in general shifted to lower temperatures, than daphniids (Bertilsson et al., 1995). Thus these two major host groups provide for their microsporidian parasites two distinct niches requiring specific biochemical and morphological adaptations which probably correspond to AOG diversification in two lineages, one predominantly composed of parasites of cyclopids and another – of daphniids (Fig. 6).

Acknowledgements

We acknowledge use of Core Microscopy Centre, School of Veterinary Medicine Louisiana State University at Baton Rouge. This research was supported by Russian Foundation for Basic Research (13-04-00693, 14-04-91176) and the Grant Council of the RF President (MD-4284.2015.4). Authors are thankful to Georgiy I. Rusakovich (Russian State University of Pedagogics named after A.I. Herzen) for his help with DNA sample processing, and to Irma V. Issi (All-Russian Institute of Plant Protection) and Igor M. Sokolov for discussions and pre-reviewing the manuscript. We are indebted to Earl Weidner (Louisiana State University) for proofreading the final version, and to two anonymous reviewers for their useful critical remarks and suggestions which essentially improved the manuscript.

Appendix A. Supplementary material

Supplementary data associated with this article can be found, in the online version, at http://dx.doi.org/10.1016/j.jip.2016.03.009.

References

Arhonditsis, G.B., Brett, M.T., 2005. Eutrophication model for Lake Washington (USA): part I. Model description and sensitivity analysis. Ecol. Model. 187, 140–178.

Bertilsson, J., Berzinš, B., Pejler, B., 1995. Occurrence of limnic micro-crustaceans in relation to temperature and oxygen. Hydrobiologia 299, 163–167.

Bronnvall, A.M., Larsson, J.I.R., 2001. Ultrastructure and light microscopic cytology of *Agglomerata lacrima* n. sp. (Microspora, Duboscqiidae), a microsporidian parasite of *Acanthocyclops vernalis* (Copepoda, Cyclopidae). Eur. J. Protistol. 37, 89–101.

Corsaro, D., Walochnik, J., Venditti, D., Steinmann, J., Müller, K.-D., Michel, R., 2014. Microsporidia-like parasites of amoebae belong to the early fungal lineage Rozellomycota. Parasitol. Res. 113, 1909–1918.

Edgar, R.C., 2004. MUSCLE: multiple sequence alignment with high accuracy and high throughput. Nucleic Acids Res. 32, 1792–1797.

Hall, T.A., 1999. BioEdit: a user-friendly biological sequence alignment editor and analysis program for Windows 95/98/NT. Nucleic Acids Symp. Ser. 41, 95–98.

Hebert, P.D.N., Penton, E.H., Burns, J.M., Janzen, D.H., Hallwachs, W., 2004. Ten species in one: DNA barcoding reveals cryptic species in the neotropical skipper butterfly *Astraptes fulgerator*. Proc. Natl. Acad. Sci. 101, 14812–14817.

James, T.Y., Pelin, A., Bonen, L., Ahrendt, S., Sain, D., Corradi, N., Stajich, J.E., 2013. Shared signatures of parasitism and phylogenomics unite cryptomycota and microsporidia. Curr. Biol. 23, 1548–1553.

Larsson, J.I.R., 1983. A revisionary study of the taxon *Tuzetia* Maurand, Fize, Fenwick and Michel, 1971, and related forms (Microspora, Tuzrtiidae). Protistologica 19, 323–355.

Larsson, J.I.R., Ebert, D., Vavra, J., 1996. Ultrastructural study of *Glugea cladocera* Pfeiffer, 1895, and transfer to the genus *Agglomerata* (Microspora, Duboscqiidae). Eur. J. Protistol. 32, 412–422.

Larsson, J.I.R., Voronin, V.N., 2000. Light and electron microscopic study of *Agglomerata volgensae* n. sp. (Microspora: Dubosqiidae), a new microsporidian parasite of *Daphnia magna* (Crustacea: Daphniidae). Eur. J. Protistol. 36, 89–99.

Larsson, J.I.R., Yan, N.D., 1988. The ultrastructural cytology and taxonomy of *Duboscqia sidae* Jirovec, 1942 (Microspora, Duboscqiidae), with establishment of the new genus *Agglomerata* gen. nov. Arch. Protist. 135, 271–288.

Navajas, M., Lagnel, J., Gutierres, J., Boursot, P., 1998. Species-wide homogeneity of nuclear ribosomal ITS2 sequences in the spider mite *Tetranychus urticae* contrasts with extensive mitochondrial COI polymorphism. Heredity 80, 742–752.

Nei, M., Kumar, S., 2000. Molecular Evolution and Phylogenetics. Oxford University Press, New York.

Ovcharenko, M., Wita, I., 2001. Ultrastructural study of *Agglomerata connexa* sp. nov. (Microspora, Duboscqiidae), a new microsporidian parasite of *Daphnia longispina* (Cladocera, Daphniidae). Acta Parasitol. 46, 94–102.

Refardt, D., Decaestecker, E., Johnson, P.T.J., Vávra, J., 2008. Morphology, molecular phylogeny, and ecology of *Binucleata daphniae* n. g., n. sp. (Fungi: Microsporidia), a parasite of *Daphnia magna* Straus, 1820 (Crustacea: Branchiopoda). J. Eukaryot. Microbiol. 55, 393–408.

Ronquist, F., Teslenko, M., Van Der Mark, P., Ayres, D.L., Darling, A., Höhna, S., Larget, B., Liu, L., Suchard, M.A., Huelsenbeck, J.P., 2012. Mrbayes 3.2: efficient bayesian phylogenetic inference and model choice across a large model space. Syst. Biol. 61, 539–542.

Sambrook, J., Fritsch, E., Maniatis, T., 1989. Molecular Cloning: A Laboratory Manual. Cold Spring Harbor Laboratories, Cold Spring Harbor, New York.

Simakova, A.V., Pankova, F.P., Tokarev, Y.S., Issi, I.V., 2005. *Senoma* gen. n., a new genus of microsporidia, with the type species *Senoma globulifera* comb. n. (syn. *Issia globulifera* Issi et Pankova 1983) from the malaria mosquito *Anopheles messeae* Fall. Protistology 4, 135–144.

Stentiford, G.D., Dunn, A.M., 2014. Microsporidia in Aquatic Invertebrates. Microsporidia: Pathogens of Opportunity,, , pp. 579–604.

Tamura, K., Peterson, D., Peterson, N., Stecher, G., Nei, M., Kumar, S., 2011. MEGA5: molecular evolutionary genetics analysis using maximum likelihood, evolutionary distance, and maximum parsimony methods. Mol. Biol. Evol. 28, 2731–2739.

Tsalolihin, S.Y., 1995. Field Guide for Invertebrates of Russia, vol. 2. Nauka, St. Petersburg, 629p..

Vávra, J., Larsson, J.I.R., 1994. *Berwaldia schaefernai* (Jírovec, 1937) comb. n. (Protozoa, Microsporida), fine structure, life cycle, and relationship to *Berwaldia singularis* Larsson, 1981. Eur. J. Protistol. 30, 45–54.

Vidtmann, S.S., Sokolova, Y.Y., 1994. The description of the new genus *Larssonia* gen. n. based on the ultrastructural analysis of *Microsporidium* (*Pleistiphora*) *obtusa* from *Daphnia pulex* (Cladocera). Parazitologiya 28, 202–213 (in Russian with English summary).

Vidtmann, S.S., Sokolova, Y.Y., 1995. A new microsporidia *Alfvenia ceriodaphniae* sp. n. from *Ceriodaphnia reticulata* (Crustacea: Cladocera). Parazitologiya 29, 214–218 (in Russian with English summary).

Voronin, V.N., 1986. The Microsporidia of crustaceans. In: Beyer, T.V., Issi, I.V. (Eds.), Protozoology: Microsporidia, vol. 10. Nauka, Leningrad, pp. 137–166 (in Russian with English summary).

Voronin, V.N., 1989. Classification of the polar filaments of microsporidia on the base of their ultrastructure. Citologia 31, 1010–1015 (in Russian with English summary).

Voronin, V.N., 1990. The effect of methods of the host preparation on the microsporidian extrasporal coat. Parazitologiya 23, 242–244 (in Russian with English summary).

Vossbrinck, C.R., Andreadis, T.G., Debrunner-Vossbrinck, B.A., 1998. Verification of intermediate hosts in the life cycles of microsporidia by small subunit rDNA sequencing. J. Eukaryot. Microbiol. 45, 290–292.

Vossbrinck, C.R., Andreadis, T.G., Vavra, J., Becnel, J.J., 2004. Molecular phylogeny and evolution of mosquito parasitic microsporidia (Microsporidia: Amblyosporidae). J. Eukaryot. Microbiol. 51, 88–95.

Vossbrinck, C.R., Debrunner-Vossbrinck, B.A., 2005. Molecular phylogeny of the Microsporidia: ecological, ultrastructural and taxonomic considerations. Folia Parasitol. 52, 131–142.

Vossbrinck, C.R., Debrunner-Vossbrinck, B.A., Weiss, L.M., 2014. Phylogeny of the Microsporidia. In: Weiss, L.M., Becnel, J.J. (Eds.), Microsporidia: Pathogens of Opportunity, first ed., pp. 203–220.

Weiss, L.M., Vossbrinck, C.R., 1999. Molecular biology, molecular phylogeny, and molecular diagnostic approaches to the microsporidia. In: Wittner, M., Weiss, L. M. (Eds.), The Microsporidia and Microsporidiosis. American Society of Microbiology, Washington, D.C., pp. 129–171.